Crossed Beam Pump and Probe Dynamics in Metal Clusters

K. Andrae,[1] P.-G. Reinhard,[1] and E. Suraud[2]

[1]*Institut für Theoretische Physik, Universität Erlangen, Staudtstrasse 7, D-91058 Erlangen, Germany*

[2]*Laboratoire de Physique Théorique, Université Paul Sabatier, 118 Route de Narbonne, F-31062 Toulouse, Cedex, France*

(Received 9 May 2003; published 30 April 2004)

We investigate theoretically pump and probe dynamics in metal clusters with crossed-polarization laser beams. We explore the relation between the pronounced Mie plasmon resonance and the laser frequency. The resonance moves with the cluster radius and splits according to the actual deformation. We demonstrate that probe pulses with different (linear) polarization axes allow one to resolve the global shape oscillations of the cluster in monopole and quadrupole degrees of freedom.

DOI: 10.1103/PhysRevLett.92.173402 PACS numbers: 36.40.Cg, 36.40.Gk, 36.40.Wa

Time resolved measurements constitute a key issue for our understanding of the dynamics of microscopic systems. Pump and probe experiments have served as a key tool to analyze a large variety of quantum dynamical processes in molecules and solids [1,2]. The successes of pump and probe spectroscopies have also motivated investigations for free clusters, experimentally [3–5] and theoretically [6]. These studies are limited to very small clusters as they still aim at a very detailed inspection of specific reaction channels, similar to molecular investigations. Time resolved spectroscopy has also started to attack larger clusters in several very promising experiments [7–10]. They provide essential information on the dynamics of gross properties, as, e.g., the dynamics of global expansion. Such investigations need to be complemented by theory at the level of microscopic modeling. There exist already a few microscopic investigations [11–13] which, however, deal with simple laser profiles. Mostly the length of the pulse is used to identify the underlying dynamical processes. We aim here at modeling the detailed pump and probe scenarios for metal clusters. A previous exploratory study investigated the effect of breathing vibrations in a spherical cluster [14]. Now we are going deeper into the detailed mechanisms and demonstrate how to disentangle the effects of the other important gross property: the dynamics of quadrupole deformation.

The tool of investigation is a coupled electronic and ionic dynamics. We take the simplest case of Na_9^+ for this principle study. One valence electron per Na ion is handled explicitly. The ion-electron coupling is described by the soft local pseudopotential of [15]. The valence electrons are treated with density functional theory at the level of the time-dependent local-density approximation (TDLDA) with the functional of [16]. Ionic dynamics is determined by classical equations of motion [molecular dynamics (MD)]. Electrons and ions are propagated simultaneously (beyond Born-Oppenheimer) constituting together a TDLDA-MD. We work with grid techniques for the description of electronic wave functions and use absorbing boundary conditions throughout [17].

The basic observable is the ionization of the clusters, i.e., the number of emitted electrons $N_{\rm esc}$. It is defined as the integrated amount of electron density absorbed at the bounds of the grid. It could be measured directly in experiment by collecting the electrons (but that is rarely done) or indirectly through collecting the charge states of the final fragments. The shape of the clusters is quantified through its root mean square extensions in the x, y, or z directions: $x_{\rm rms} = \sqrt{\langle x^2\rangle - \langle x\rangle^2}$, where $\langle\ldots\rangle$ is the average over ionic positions, or electronic density, respectively. The root mean square radius of the cluster is composed as $r_{\rm rms} = \sqrt{x_{\rm rms}^2 + y_{\rm rms}^2 + z_{\rm rms}^2}$. We also consider the electronic dipole moment $\langle\mathbf{r}\rangle$ as an indicator for the dipole response (associated with surface plasmon oscillations).

The basic idea for pump and probe analysis of global shapes in metal clusters exploits the close relation between shape and the Mie surface plasmon resonance. Global expansion redshifts the frequency $\omega_{\rm res} \propto r_{\rm rms}^{-3/2}$ [18,19]. The difference between ionic and electronic radius is usually small due to the Coulomb force. Quadrupole deformation yields a splitting of the resonance such that the longer axis is related to the lower frequency, while the shorter axis is related to the higher frequency, i.e., $\omega_y - \omega_x \propto x_{\rm rms}^2 - y_{\rm rms}^2$ and similarly for the other combinations. Ionic motion will yield vibrating shapes and subsequently $\omega_x(t)$, $\omega_y(t)$, and $\omega_z(t)$. The strategy now is to place the laser frequency $\omega_{\rm laser}$ safely below all expected $\omega_{x,y,z}$. The response of the cluster is the larger the closer $\omega_{x,y,z}$ comes to $\omega_{\rm laser}$ and vice versa. Large dipole response is identified by large electron emission. Thus one can read off the ionic shape vibrations from a varying response to the probe signal, as was done successfully for pure radius vibrations in [14]. Here we go one step further and check the probe signal for three different laser polarizations, along x, y, and z. This should allow one to access the quadrupole vibrations of the cluster.

The scenario is, in fact, a bit more involved. Free clusters in an ensemble of given temperature T will undergo thermally activated rotational motion, which in

turn leads to a rotational diffusion of an initially given orientation. The diffusion time is related to the average rotational motion. It can be stretched by going to low temperatures. For example, the average time for one rotational cycle in an ensemble of Na_9^+ clusters at $T = 20$ K is about 60 ps. The rotational drift up to an angle of 10° then takes about 1.7 ps, the observation time used in this Letter. It leaves sufficient time to map the ionic vibrations. The rotational time scales with temperature as $T^{-1/2}$ and with system size as $N^{5/6}$. Anyway, very low T is required. The rotational diffusion is much too fast, e.g., for an ensemble at room temperature. This means that such experiments on free clusters are extremely demanding. Angular resolution is much better maintained in practice for clusters deposited on a surface. The basic mechanisms are the same in both cases. The following discussion of a free cluster (actually at $T = 0$) applies to both cases.

We chose Na_9^+ as a test case. It is nearly spherical initially and develops sizable quadrupole deformations after pump excitation. This simplifies the analysis because (i) the starting point provides comparable Mie plasmon frequencies in all three directions and (ii) the Mie plasmon peak is not so much perturbed by Landau fragmentation as it happens in larger clusters [19]. We start from the fully relaxed ground state of Na_9^+, with a Mie plasmon frequency at 2.7 eV. Pump and probe pulses are chosen to have the same parameters: frequency 2.3 eV, $\sin^2$ profile with FWHM of 24 fs, and intensity of 1.3×10^{10} W/cm^2 (field strength $eE = 0.0012$ Ry/a_0). Note that the laser frequency stays sufficiently far below resonance and that the intensity is in a moderate regime where resonance frequencies still play a role [20]. The symmetry axis of Na_9^+ is chosen as the z axis. We apply in the test case here the pump pulse along the x axis and the probe pulses in all three directions.

Figure 1 demonstrates the principle procedure. The pump pulse is active during the first 48 fs. Direct electron emission yields almost immediately an initial extra ionization N_{esc} [see Fig. 1(c)]. The thus created Coulomb pressure drives the ionic distribution to a different shape. The ionic response to the initial pump is exemplified in Fig. 1(a). We see oscillations of x_{rms} with typical ionic frequency [21], overlayed with a slight global expansion. The oscillations have an amplitude of only 10% of the radius.

The effect of probe pulses is demonstrated in Fig. 1(b) showing the envelope of the dipole amplitude. The first peak corresponds to the pump pulse. It perfectly maps the laser profile because we are in an off-resonant situation [22]. The same holds for the three selected probe pulses whose peaks are clearly visible. The probe peaks have different heights although the laser has always the same intensity. This indicates a different strength of response. Figure 1(c) shows with the same line types the electron emission N_{esc} triggered by the response. The amount of extra emission is clearly related to the amplitude of the dipole response. The kind of detailed plotting as done in Fig. 1 here becomes fuzzy when considering a dense succession of probe pulses. In the following, we concentrate on the net effect of the probes. We draw the maximum of the dipole peak and the net emission 48 fs after the end of the pulse, both versus probe time.

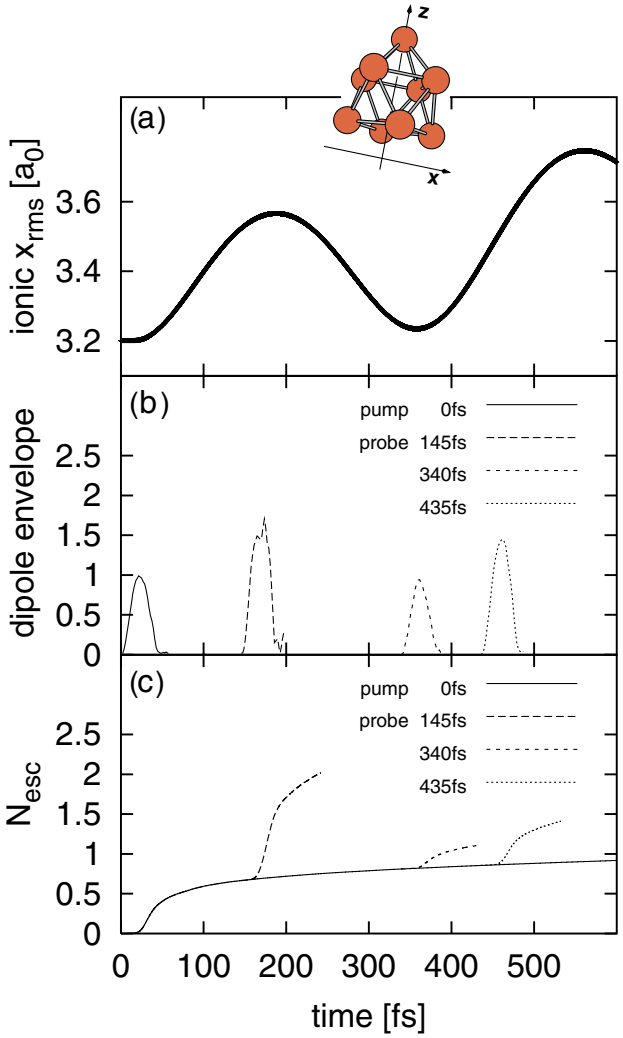

FIG. 1 (color online). Demonstration of pump and probe analysis for Na_9^+. The laser parameters are as follows: frequency $\omega = 2.3$ eV; intensity 1.3×10^{10} W/cm^2; the profile is a $\sin^2$ pulse with FWHM = 24 fs; polarization is in the x direction (orthogonal to symmetry axis). The pump pulse was active in the first time bin 0–48 fs. Panel (a) shows the ionic rms radius for free evolution after pump. Panels (b) and (c) show the effect of a three probe pulse applied at different delay times, with (b) the envelope of dipole momentum in the x direction and (c) the number of emitted electrons in the course of time.

Figure 2 is the main result of our pump and probe analysis. It summarizes data from a dense series of probe pulse and for all three polarizations. Figure 2(a) shows the time evolution of ionic x_{rms}, y_{rms}, and z_{rms} after the pump pulse. All three directions oscillate with about similar frequencies. The overlayed slower trends differ. The cluster starts from the slightly prolate ground state

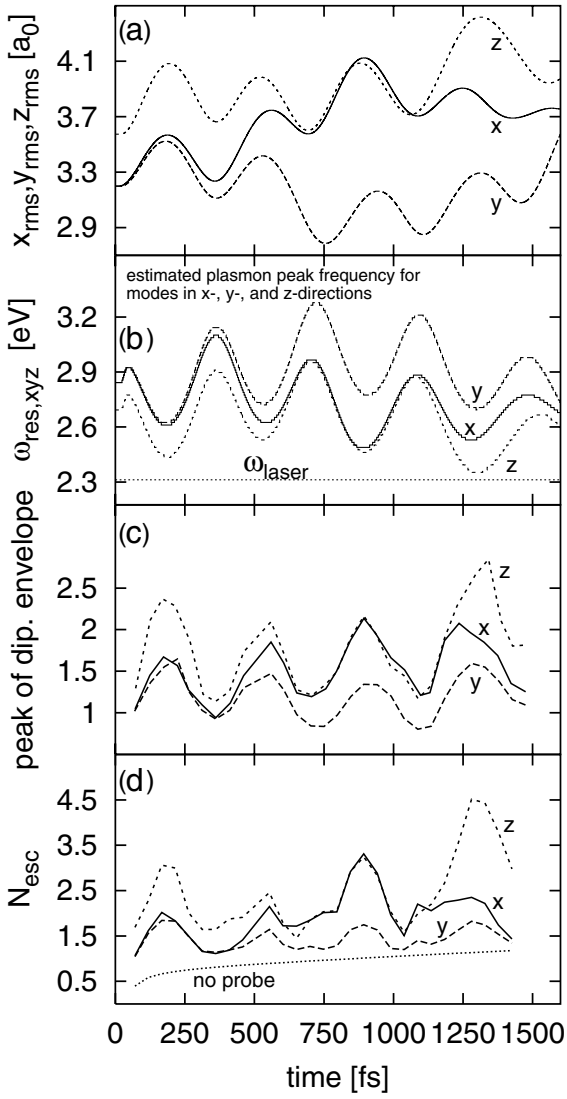

FIG. 2. Time evolution of key observables in a pump and probe analysis of Na_9^+. The laser parameters are as given in Fig. 1. The pump pulse was active in the first time bin 0–48 fs. Panels (a) and (b) show features of the free evolution after pump, with (a) the rms extensions in the x, y, and z directions and (b) the estimated plasmon peak frequency for modes in the x, y, and z directions plus a horizontal dashed line to indicate the laser frequency. The probe pulses are applied in successive time bins of 48 fs. Panels (c) and (d) show features of the probe, with (c) the maximum amplitude of dipole response and (d) the number of emitted electrons after probe (fine dotted line without probe).

configuration (same x and y with somewhat larger z). The x_{rms} expands in the first 1000 fs relative to the two others. This causes triaxial shapes around 400 fs and reaches an oblate configuration at 750 fs. Triaxial shapes reappear later at around 1250 fs. It is interesting to note that the evolution of x_{rms} makes here, in Fig. 2, a different impression than in Fig. 1. The observation over a longer time and combined view with the two other directions shows that we see a slow oscillation between different shapes rather than a global expansion. Figure 2(b) shows an estimate of the Mie plasmon frequencies deduced in a collective picture from the given rms extension and the actual net charge $1 + N_{esc}(t)$. The dependence on r_{rms} and on x_{rms}, y_{rms}, and z_{rms} was discussed above. The base frequency depends on N_{esc} as $\omega_0 = 0.205\,\mathrm{Ry}(1 + 0.025 N_{esc})$. The deformation splitting is added on top. (All trends were evaluated in a deformed jellium model [19,23] and counterchecked for a few detailed ionic configurations here.) The laser frequency is drawn for comparison. We see that the Mie frequencies follow the reciprocal trends of the rms extensions. The probe frequency stays always below resonance. The difference frequency varies dramatically. Figure 2(c) shows the dipole response to the probe pulses (peak amplitude at probe time) for the three different polarizations along the x, y, and z directions. Comparison with Fig. 2(b) shows that response is large for low Mie frequency and small for the large one. This, in turn, means large dipole response for large extension [Fig. 2(a)]. Figure 2(d) shows the N_{esc} after the probe pulses in three different polarization directions. It maps perfectly the dipole response and with it the time evolution of x_{rms}, y_{rms}, and z_{rms}. Having that signal for the three separate directions at hand, one can directly read off the changes in deformation, from prolate over triaxial to oblate and back. The basic message of Fig. 2 is comprised by comparison of Fig. 2(a) with Fig. 2(d): time resolved measurement of N_{esc} with specific probe-pulse polarization is directly related to the global ionic extension in the x, y, and z directions.

It is now clear that one can identify the ionic quadrupole dynamics from probe pulses at different polarizations. The question is whether one can retrieve also a signal on the global extension (monopole). One suspects that an average over the three polarization axes could provide that. The upper panel of Fig. 3 shows the N_{esc} averaged over the three polarization axes. This is to be compared with the rms radius shown in Fig. 3(b). It is obvious that the average emission maps fairly well the radius of the cluster.

Figures 3(c) and 3(d) show complementary information on the time evolution of the electron distribution after the pump pulse. The electronic radius [Fig. 3(c)] shows a sharp initial spike. It reflects the dipole response to the pump pulse. After the pulse is over, the electronic radius nicely follows the oscillations of the ionic radius. Figure 3(d) shows the x_{rms}, y_{rms}, and z_{rms} separately. All three have the spike from the pump pulse. And after that, the electronic extensions show the same pattern as the ionic ones [Fig. 2(a)]. This demonstrates once more that the Coulomb force tries to keep electronic and ionic distributions aligned even under these hefty dynamic conditions.

Altogether, we have considered a particular scenario for pump and probe experiments in metal clusters: the cluster was chosen to have a clean Mie plasmon peak with initially little fragmentation or deformation splitting. The

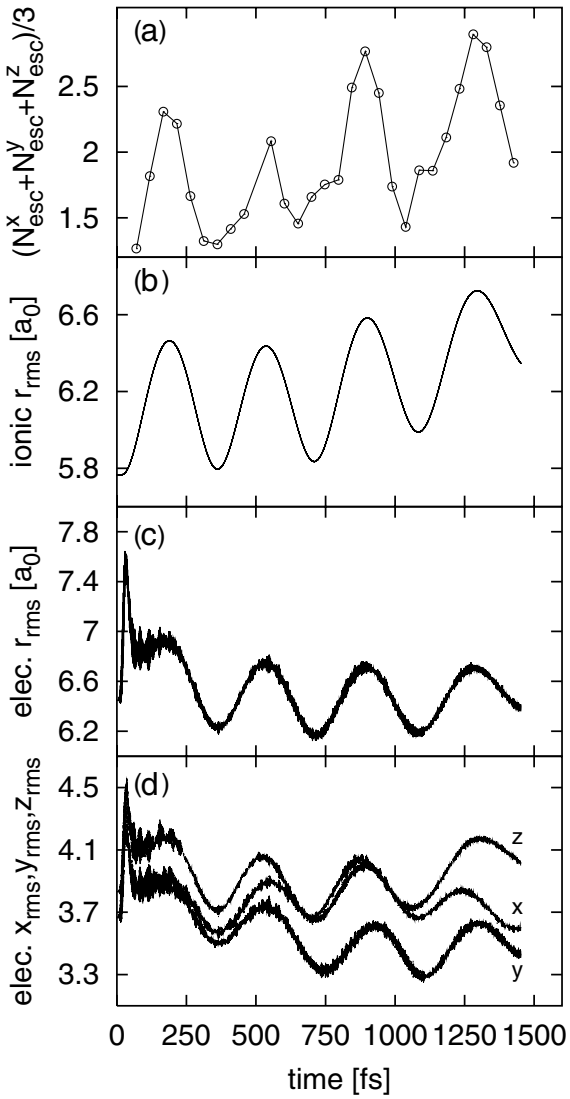

FIG. 3. Complementing information for pump and probe analysis of Na_9^+. Panel (a) shows the number of emitted electrons after probe averaged over all three polarization directions, (b) the ionic rms radius for free evolution after pump, (c) the electronic rms radius for free evolution, and (d) the separate electronic x, y, and z extensions for free evolution after pump. The laser parameters are as given in Fig. 1.

laser frequency for pump and probe was chosen a certain amount below the Mie resonance, far enough to avoid direct resonant conditions for all cluster shapes of interest and not too far to maintain sensitivity to the resonance frequency. In the actual example we have used $\omega_{\text{laser}} = 2.3$ eV for an initial Mie plasmon frequency of 2.7 eV. The intensity is chosen such that the pump probe leads to emission of about one electron, lifting the charge state of Na_9^+ by about one. This system stays stable for a sufficiently long time (at least a few ps) but exhibits sizable oscillations of the ionic shape. These shape changes can be explored by the probe pulses using the final electron emission as signature. By varying the polarization of the probe pulse in three orthogonal directions, one can nicely map the time evolution of the global shape in terms of radius and of quadrupole moment. This is a very promising result as it demonstrates the possibility of time resolved spectroscopy of the collective vibrations in metal clusters. As discussed above, the case of free clusters requires very low temperatures in a practical measurement. Experimentally more accessible is the case of deposited clusters in which such cross beam experiments should be in reach. The above considerations apply to that case as well.

The scenario studied here was designed to give simple and robust access to global properties. A world of different scenarios is conceivable. Most of them would be able to look specifically to this or that detailed cluster property. This requires, in turn, that much more knowledge of a particular cluster has to be invested before one can deduce unambiguously more subtle features as, e.g., secondary resonances or single particle states. A rich field of research is opening up and the robust strategy proposed here is probably a possible first step.

This work has been supported by the French-German exchange program PROCOPE, Contract No. 99074, and by Institut Universitaire de France.

[1] A. H. Zewail, *Femtochemistry* (World Scientific, Singapore, 1994), Vols. I & II.
[2] B. M. Garraway *et al.*, Rep. Prog. Phys. **58**, 365 (1995).
[3] K. Ertel *et al.*, Appl. Phys. B **68**, 439 (1999).
[4] T. Leisner *et al.*, J. Chem. Phys. **111**, 1017 (1999).
[5] R. Heinicke and J. Grotemeyer, Appl. Phys. B **71**, 419 (2000).
[6] M. Hartmann *et al.*, J. Chem. Phys. **108**, 3096 (1998)
[7] L. Köller *et al.*, Phys. Rev. Lett. **82**, 3783 (1999).
[8] G. Seifert *et al.*, Appl. Phys. B **71**, 795 (2000).
[9] J. Zweiback *et al.*, Phys. Rev. Lett. **84**, 2634 (2000).
[10] D. A. Card *et al.*, J. Chem. Phys. **116**, 3554 (2002).
[11] M. E. Garcia, Appl. Phys. A **72**, 261 (2000).
[12] C. Siedschlag and M. Rost, Phys. Rev. Lett. **89**, 173401 (2002).
[13] E. Suraud *et al.*, Phys. Rev. Lett. **85**, 2296 (2000).
[14] K. Andrae *et al.*, J. Phys. B **35**, 4203 (2002).
[15] S. Kümmel *et al.*, Eur. Phys. J. D **9**, 149 (1999).
[16] J. P. Perdew and Y. Wang, Phys. Rev. B **45**, 13 244 (1992).
[17] F. Calvayrac *et al.*, Phys. Rep. **337**, 493 (2000).
[18] M. Brack, Rev. Mod. Phys. **65**, 677 (1993).
[19] P.-G. Reinhard *et al.*, Ann. Phys. (Leipzig) **5**, 576 (1996).
[20] P.-G. Reinhard *et al.*, Eur. Phys. J. D **3**, 175 (1998).
[21] P.-G. Reinhard and E. Suraud, Eur. Phys. J. D **21**, 315 (2002)
[22] C. A. Ullrich *et al.*, J. Phys. B **30**, 5043 (1997).
[23] B. Montag and P.-G. Reinhard, Phys. Rev. B **51**, 14 686 (1995).